for isozyme III, very strong anion binding is reported.[3] Isozyme III has a much more positive potential in the active site region that would enhance anion binding. The model is so simple that it is easy to suggest that water or other nearby ionic residues or couples such as the Thr–Glu will alter details. It does show the need for the more complete treatment exists and that all of the studies of CA have not properly considered the problem of the ionicity of the metal active site.

Registry No. Carbonic anhydrase, 9001-03-0.

Zeolites versus Aluminosilicate Clusters: The Validity of a Local Description

G. J. Kramer,*,† A. J. M. de Man,‡ and R. A. van Santen†,‡

Contribution from the Koninklijke/Shell-Laboratorium, Amsterdam (Shell Research B.V.), P.O. Box 3003, 1003 AA Amsterdam, The Netherlands, and Laboratory of Inorganic Chemistry and Catalysis, Schuit Institute of Catalysis, Eindhoven University of Technology, P.O. Box 513, 5600 MB Eindhoven, The Netherlands. *Received December 7, 1990*

Abstract: A comparison of force field calculations on extended systems and ab initio quantum chemical calculations on ring structures reveals that the relative energy content of neutral-framework silicas and aluminophosphates is determined by that of the smallest substructures. Energy-minimized structures containing only four, five, and six rings have the same energy content to within 10 kJ/mol. Hypothetical three-ring-containing structures have considerably higher energy content, which may well inhibit their synthesis in the pure SiO_2 modification. The results accord with sparse experimental information. Using the same combination of techniques, we demonstrate that substitution of aluminum in silica causes an appreciable, albeit local, distortion of the lattice. The relaxation energy for such a substitution amounts to 100–200 kJ/mol, depending on the way charge compensation is accomplished.

1. Introduction

Secondary building units (SBU) play an important role in the structural study of zeolites and aluminophosphates. The SBUs are small composite entities like rings or double rings, built from corner sharing TO_4 (T = Si, Al, P) tetrahedrons, which can be used to formally describe the framework topology.[1] Thus, they provide a useful tool for classifying the large number of known zeolite networks as well as for systematically enumerating the endless number of hypothetical four-connected networks.[2-4] At a less abstract level, their proven existence in silica synthesis gels[5,6] has led to speculations concerning their role in steering the still poorly understood process of zeolite synthesis.[7-10]

Lastly, SBUs are very similar to the clusters that are used by theoretical chemists as model systems for zeolites, in studies on zeolite stability,[11] acidity,[12,13] water coordination,[14] and framework substitutions.[15-17] The use of ab initio quantum chemical calculations on these small clusters contrasts with the other approach of zeolite theoretical chemistry: the classical modeling of extended systems, using force fields to describe the interactomic interactions.[18,19] So far it has been difficult to reconcile the two theoretical approaches.

Force field methods are suited to deal with extended structures built from large unit cells. However, since they are based on effective, classical potentials, they are not able to handle electronic effects that control the chemical reactivity of isomorphously substituted zeolites. The theoretical study of the acidity of protons attached to a zeolite lattice provides an example of such a problem. This kind of subject can at present only be approached by application of quantum chemical calculus to small clusters. The variational character of the ab initio SCF scheme of quantum chemistry implies that the results are unambiguous only for geometry-optimized clusters.[20] The question that emerges is whether or not, or to what extent, the results on geometry-optimized (free) clusters still have any bearing on the chemically reactive sites embedded in extended systems (zeolites), where the geometric freedom of the cluster is restricted.

In this paper, we will explore the extent to which zeolitic substructures can still be considered free building blocks, when embedded in the extended zeolite. To this end, we employ both ab initio quantum chemical tools and force field methods. The force field that will be used is based on the parametrization of

† Koninklijke/Shell-Laboratorium, Amsterdam.
‡ Eindhoven University of Technology.

(1) Meier, W. M.; Olsen, D. H. *Atlas of Zeolite Structure Types*, 2nd revised ed.; Butterworth: Cambridge, 1987.
(2) Barrer, R. M. *Zeolite and Clay Minerals as Sorbents and Molecular Sieves*; Academic Press: London, 1978.
(3) Smith, J. V. *Am. Mineral.* **1977**, *62*, 703–709. *Ibid.* **1978**, *63*, 960–969. *Ibid.* **1979**, *64*, 551–562.
(4) Meier, W. M. In *New Developments in Zeolite Science and Technology*; Murakumi, Y., et al., Eds.; Studies in Surface Science and Catalysis 28; Elsevier: Amsterdam, 1986; pp 13–22.
(5) Groenen, E. J. J.; Kortbeek, A. G. T. G.; Mackay, M.; Sudmeijer, O. *Zeolites* **1986**, *6*, 403.
(6) Kinrade, S. D.; Swaddle, T. W. *Inorg. Chem.* **1988**, *27*, 4253–4259.
(7) Van Santen, R. A.; Keijsper, J.; Ooms, G.; Kortbeek, A. G. T. G. In *New Developments in Zeolite Science and Technology*; Murakumi, Y., et al., Eds.; Studies in Surface Science and Catalysis 28; Elsevier: Amsterdam, 1986; pp 169–175.
(8) Szostak, R. *Molecular Sieves, Principles of Synthesis and Identification*; Van Nostrand Reinhold: New York, 1989; see also references therein.
(9) Dent-Glasser, L. S.; Lachowski, E. E. *J. Chem. Soc., Dalton Trans.* **1980**, 399.
(10) Knight, C. T. G. *Zeolites* **1990**, *10*, 140–144 and references therein.
(11) Van Beest, B. W. H.; Verbeek, J.; Van Santen, R. A. *Catal. Lett.* **1988**, *1*, 147–154.
(12) Sauer, J.; Kölmel, C. M.; Hill, J. R.; Ahlrichs, R. *Chem. Phys. Lett.* **1990**, *164*, 193–198.
(13) Beran, S. *J. Phys. Chem.* **1990**, *94*, 335–337.
(14) Sauer, J.; Horn, H.; Häser, M.; Ahlrichs, R. *Chem. Phys. Lett.* **1990**, *173*, 26–32.
(15) Fripiat, J. G.; Galet, P.; Delhalle, J.; André, J. M.; Nagy, J. B.; Derouane, E. G. *J. Phys. Chem.* **1985**, *89*, 1932–1937.
(16) Derouane, E. G.; Fripiat, J. G. *Zeolites* **1985**, *5*, 165–172.
(17) O'Malley, P. J.; Dwyer, J. *Zeolites* **1988**, *8*, 317–321.
(18) Van Santen, R. A.; Ooms, G.; Den Ouden, C. J. J.; Van Beest, B. W. H.; Post, M. F. M. *Zeolite Synthesis*; ACS Symposium Series 398; American Chemical Society: Washington, DC, 1989; pp 617–633.
(19) Jackson, R. A.; Catlow, R. C. A. *Mol. Simul.* **1988**, *1*, 207–224.
(20) Hehre, W. J.; Radom, L.; Schleyer, P. v. R.; Pople, J. A. *Ab Initio Molecular Orbital Theory*; John Wiley & Sons: New York, 1986; p 92.

0002-7863/91/1513-6435$02.50/0

Table I. Total Energies (hartrees/Si) and Energy Differences (kJ/mol Si) of Optimized Silica Clusters as Obtained from ab Initio Quantum Chemistry[a]

SBU	symm	STO3G		3-21G	
		E	δE	E	δE
6	C_{6v}	-508.415 799[b]	0		
5	C_{5v}	-508.415 783[b]	0.0	-512.157 759	0
4	C_{4v}	-508.415 471[b]	0.9	-512.156 219	4.0
3	C_{3v}	-508.412 064[b]	9.8	-512.146 629	29.2
4^6	O_h	-470.900 205	0		
3^4	T_d	-470.885 809	37.8		
4^66^8	O_h			-474.371 00[c]	0
4^66^2	D_{6h}			-474.370 18[c]	2.2
3^4	S_4			-474.332 22	101.8

[a] SBUs are denoted by their Schläfli symbols (e.g., 4^66^2 is a double-six-ring structure). [b] From ref 11. [c] From ref 26.

the energy surface of small zeolitic clusters, determined from ab initio calculations. At the same time, we have ascertained that it accurately describes the structure and properties of extended systems. This force field and the philosophy behind it have been elaborated in two previous papers.[21,22]

This dual approach will be used to study two types of systems. Firstly, we will study the relative energies of all-silica zeolites and all-silica clusters. It appears that the energy of a zeolitic SiO_2 polymorph can be considered to be the sum of the energies of clusters (specifically rings), indicating that the strain that arises from the embedding of free ring structures into the infinite lattice is small (less than 10 kJ/mol SiO_2). The small energy differences found between SiO_2 systems with different network topologies is in quantitative agreement with the sparse experimental information about this subject.[23] Also, we find that three-ring molecular sieves have a considerably higher energy content, which may prohibit their synthesis (at least in the purely silaceous form). The same invariance of the energy for differences in network topology is found for $AlPO_4$ polymorphs. Here three-ring structures are forbidden because of the alternation of Al and P within the framework.

In a second series of calculations, we will extend the scope to aluminosilicates, focusing on the local properties of an isolated aluminum substituted into the framework of a SiO_2 zeolite. The local environment of such a substitution is of particular interest, since it is thought responsible for the catalytic behavior of aluminosilicates in heterogeneous catalysis. For this system, as for the all-silica system, the strain that results from replacement of silicon by aluminum (having a 0.1 Å longer bond to oxygen) is removed by structure relaxation in zeolites and clusters alike. This provides support for the idea that small geometry-optimized clusters are suited for studying the acidic properties of extended zeolites.

In the next section, we will present the details of both the quantum chemical calculations and the lattice energy minimization calculations. Also, we point out how an effective interaction potential for an acidic OH group was derived from ab initio calculations on a small cluster. Finally, a scheme is presented for the correction of force field energies for a spurious density dependence. An analysis and a detailed comparison of ab initio and force field results are reserved for the Discussion. In the Conclusion, results and their implications are summarized.

2. Computational Details and Results

2.1. Quantum Chemical Calculations. Quantum chemical calculations were performed with the GAMESS ab initio package,[24] using either STO3G minimal basis set or the 3-21G split valence basis. The systems chosen for these calculations can be considered to be secondary building blocks of zeolites: three-, four-, five-, and six-ring structures and the double-four-ring structure (4^6). Also, a supertetrahedron (3^4) was considered, built from four SiO_4 tetrahedra. This type of unit has been observed in the new germanium sulfide molecular sieves,[25] and is analogous to the building blocks for very large pore zeolites that were proposed by Meier.[4] Supplementary information on double-six-ring units (4^66^2) and the sodalite unit (4^66^8) was taken from the literature.[26]

All clusters were terminated with OH groups, ensuring the proper 4-coordination with oxygen of the silicon atoms. For all systems, the geometry was optimized with the restriction that the symmetry be retained. The symmetry, energy, and relative energy of the clusters are given in Table I. Note that four-, five-, and six-ring structures have virtually the same energy content, while three-ring structures have an energy content that is 10–30 kJ/mol higher.

Finally, the relaxation energy of an aluminum substitution in a free silica ring was calculated at the 3-21G SCF level. As a reference, the geometry-optimized structure of an all-silica four-ring structure in D_{4h} symmetry was used. This cluster will be denoted as 4R-Si. Three models have been used to study the effect of aluminum substitution in this ring: In the first model, silicon is exchanged with aluminum, rendering the cluster negatively charged. In the second and the third models, the

Table II. Total Energies (hartrees) of Ring-Shaped Aluminosilicate Clusters at the 3-21G SCF Level in the All-Silica Geometry and Geometry-Optimized[a]

SBU	symm	E (au)	
		all-Si geometry	optimized geometry
4R-Si	D_{4h}	-2048.603 11	
4R-Al	D_{2h}	-2001.807 12	-2001.850 64
4R-AlNa	D_{2h}	-2162.748 18[b]	-2162.797 39
4R-AlO_H	C_s	-2002.293 79[c]	-2002.374 32

[a] The point group symmetry of the clusters is also indicated. [b] Na^+ position optimized. [c] Proton position optimized.

Table III. Bonding Distances (Å) and Angles of the $(OH)_3Si$–(OH)–$Al(OH)_3$ Dimer, Found from ab Initio Calculations, Compared with the Averaged Distances and Angles Found from Force Field Calculations on a Single Al/OH Substitution in Faujasite[a]

bond	ab initio		force field	
SiO	4R-Si	1.620	FAU-Si	1.61 ± 0.01
SiOSi		162.8		153 ± 6
SiO	4R-Al	1.613	FAU-Al	1.61 ± 0.01
$Si_{NN}O$		1.639		1.62 ± 0.01
$Si_{NN}O_{NN}$		1.588		1.56 ± 0.01
AlO		1.736		1.69 ± 0.02
SiOSi		159.4		153 ± 6
SiOAl		161.7		146 ± 5
SiO	4R-AlNa	1.618	FAU-AlNa	1.61 ± 0.01
$Si_{NN}O$		1.629		1.62 ± 0.01
$Si_{NN}O_{NN}$		1.608		1.58 ± 0.01
AlO		1.706		1.69 ± 0.04
AlNa		2.823		2.78
ONa		2.071 (2×)		2.22 (2×)
SiOSi		162.8		153 ± 7
SiOAl		158.6		144 ± 15
SiO	4R-AlO_H	1.62 ± 0.01	FAU-AlO_H	1.61 ± 0.01
$Si_{OH}O$		1.591		1.56 ± 0.01
$Si_{OH}O_H$		1.698		1.70 ± 0.02
AlO		1.685		1.60 ± 0.01
AlO_H		1.895		2.10 ± 0.06
$OSiO_H$		109.1		102 ± 5
$OAlO_H$		104.1		93 ± 4
SiOSi		163 ± 22		153 ± 7
SiO_HAl		140.0		134 ± 5

[a] The latter figures are averages over all possible O_H substitution sites. The subscript NN denotes nearest neighborship to the Al substituent; Si_{OH} denotes Si atoms connected to an OH group.

(21) Van Beest, B. W. H.; Kramer, G. J.; Van Santen, R. A. *Phys. Rev. Lett.* **1990**, *64*, 1955–1958.
(22) Kramer, G. J.; Farragher, N. P.; Van Beest, B. W. H.; Van Santen, R. A. *Phys. Rev. B* **1991**, *43*, 5068–5080.
(23) Johnson, G. K.; Tasker, I. R.; Howell, D. A.; Smith, J. V. *J. Chem. Thermodyn.* **1987**, *19*, 617.
(24) Dupuis, M.; Sprangler, D.; Wendolowski, D. *NRCC Software Catalog* **1980**, *1*, Program No. QG01, GAMESS. Guest, M. F.; Kendrick, J. *GAMESS User Manual, An Introductory Guide*; Daresbury Laboratory: Warrington, UK, 1986; CCP/86/1.
(25) Bedard, R. L.; Wilson, S. T.; Vail, L. D.; Bennett, J. M.; Flanigen, E. M. In *Zeolites: Facts, Figures, Future*; Jacobs, P. A., et al., Eds.; Studies in Surface Science and Catalysis 49; Elsevier: Amsterdam, 1990; pp 375–387.
(26) Ahlrichs, R.; Bär, M.; Häser, M.; Kölmel, C.; Sauer, J. *Chem. Phys. Lett.* **1989**, *164*, 199–204.

Table IV. Force Field Parameters for Si, Al, P, O, Na, and O_H[a]

species α_i–α_j	short-range parameters $A_{\alpha_i\alpha_j}$ (eV)	$b_{\alpha_i\alpha_j}$ (Å^{-1})	$C_{\alpha_i\alpha_j}$ (eV Å^6)	charges q_α
O–O	1388.7730	2.760 00	175.0000	q_O = −1.20
O–O_H	9747.0105	3.879 92	175.0000[b]	q_{O_H} = −0.20
O_H–O_H			175.0000	
Si–O	18 003.7572	4.873 18	133.5381	q_{Si} = 2.40
Si–O_H	26 949.7285	5.038 88	176.6941	
Al–O	15 430.4434	4.815 06	130.8516	q_{Al} = 1.40
Al–O_H	9419.8585	4.510 28	102.8589	
P–O	9034.2080	5.190 98	19.8793	q_P = 3.40
Na–O	3542.2072	4.134 55	0.0000	q_{Na} = 1.00
Si–O_H–Al	k = 0.5334 eV·rad^{-2}, θ_0 = 88.62°			
O–O	1388.7730	2.760 00	175.0000	q_O = −1.20
O–O_H	37 139.8950	4.655 93	175.0000[b]	q_{O_H} = −0.70
O_H–O_H			175.0000	
Si–O	18 003.7572	4.873 18	133.5381	q_{Si} = 2.40
Si–O_H	14 031.8388	4.790 34	101.0583	
Al–O	8566.5434	4.662 22	73.0913	q_{Al} = 1.90
Al–O_H	3237.5079	4.053 60	32.2857	
Si–O_H–Al	k = 0.7099 eV·rad^{-2}, θ_0 = 88.42°			
O–O	1388.7730	2.760 00	175.0000	q_O = −1.20
Si–O	17 841.7551	4.870 84	132.3647	q_{Si} = 2.41
Al–O	8149.8485	4.647 34	69.4411	q_{Al} = 1.93
O–O	1388.7730	2.760 00	175.0000	q_O = −1.20
Si–O	17 679.5856	4.868 48	131.1889	q_{Si} = 2.42
Al–O	14 630.3317	4.802 87	124.2818	q_{Al} = 1.46

[a] The symbol O_H refers to an effective atom representing a protonated oxygen. The force fields between blank lines form internally consistent sets. The first uses a formal charge *difference* (δQ = 1.00). The subsequent sets are for δQ = 0.50, 0.96, and 0.48. Fixed during optimization.

negative charge is balanced by a sodium ion and a proton, respectively. For all models, we started with the all-silica geometry of the cluster. For the second and third models, the Na^+ and the proton position were optimized, respectively. Next, a complete geometry optimization was performed, giving the ideal geometry of the free cluster and the relaxation energy. The energies and symmetries of the clusters are given in Table II. Relevant structural parameters are listed in Table III.

2.2. Ab Initio Force Field. The derivation of a force field to describe the interatomic interactions within (alumino)silicates and aluminophosphates from quantum mechanical ab initio calculations and its testing have been described in two previous papers.[21,22] The potential energy function ϕ_{ij} for the interaction of atoms i and j is of the form

$$\phi_{ij}(r_{ij}) = \frac{q_i q_j}{r_{ij}} + A_{ij}\exp(-b_{ij}r_{ij}) - \frac{c_{ij}}{r_{ij}^6} \qquad (1)$$

where q_i (q_j) denotes the effective charge of atom i (j); A_{ij}, b_{ij} and c_{ij} are short-range parameters that depend on the atomic species of i and j. Its functional form—a Buckingham-type short-range interaction plus Coulomb interaction—is of the type often used to model silicates.[19,27] All force field parameters were adjusted to fit both the ab initio determined potential energy surface of small clusters and the structural and elastic properties of simple crystal structures, thereby assuring their validity both at microscopic and macroscopic level. Force field parameters are given in Table IV.

While the functional form of eq 1, with suitably chosen parameters, allows accurate prediction of silicate properties,[22] one should bear in mind that force fields are ultimately empirical and no direct physical meaning can be given to either one of the parameters. Specifically, the constants of the r^{-6} attraction terms (c_{ij}) are not related to the van der Waals interaction between nonbonded atoms. Rather, they serve a dual purpose of (i) determining the bonded interactions between neighboring atoms and (ii) modifying the Coulomb interactions at intermediate distances, typically between next-nearest and second-nearest neighbors. As we will see in section 2.4, the empirical nature may in some cases lead to artifacts, for which a correction has to be introduced.

In order to provide for modeling of protonated aluminosilicates, we have extended the force field with force field parameters for an OH group. This group is treated as an effective atom, denoted as O_H, centered at the oxygen position. Its force field parameters were derived from

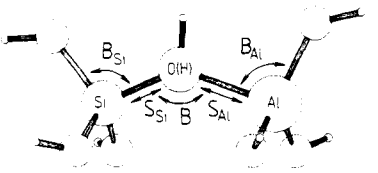

Figure 1. $(OH)_3Si$–(OH)–$Al(OH)_3$ dimer. The bending (B) and stretching (S) modes used to construct the potential energy surface are also indicated.

Table V. Bond Distances (Å) and Bond Angles (degrees) of the Geometry-Optimized $(OH)_3Si$–(OH)–$Al(OH)_3$ Dimer[a]

bond	distance/angle
SiO	1.611
SiO_H	1.670
AlO	1.714
AlO_H	1.995
O_HH	0.960
SiO_HAl	138.8
$OSiO_H$	106.6
$OAlO_H$	99.4

[a] The assumed symmetry in C_s.

the potential energy surface of a $(OH)_3Si$–(OH)–$Al(OH)_3$ dimer (Figure 1). This potential energy surface was calculated at the RHF-SCF level, using the valence part of the 6-31G* basis and employing effective core potentials for the core electrons.[21] Relevant distances, angles, and Mulliken populations of the geometry-optimized dimer are given in Table V. Note that the Al–O_H[28] bond length is significantly larger than the regular Al–O distance. This is accompanied by a significant reduction of the O_H–Al–O angle with respect to the tetrahedral angle. Similar distortions are reported in the literature.[12,14]

Starting from the geometry-optimized structure (see Table III), the potential energy surface was sampled for four different distortion modes drawn in Figure 1. The Si–O and Al–O bond lengths were varied from 1.35 to 1.95 and from 1.55 to 2.15 Å, respectively, the O–Si–O_H and O–Al–O_H angles between 70 and 130°, and the Si–O_H–Al angle between 120 and 160°. For each configuration of the $(OH)_3Si$–(O)–$Al(OH)_3$ backbone, the hydrogen position within the bridging hydroxyl group was optimized. The optimization of the hydrogen position is imposed by the effective atom approach: We implicitly assume that the proton position is always ideal, i.e., not hindered by geometrical constraints of, e.g., the zeolite lattice. The O–O_H interaction was determined from the O–T–O_H bending modes. Subsequently, the Si–O_H and Al–O_H interaction could be determined from the stretching modes.

It appeared to be necessary to include a bond bending term to account for the rigidity of the Si–O_H–Al angle. The 3-coordination of oxygen in a bridging hydroxyl group results in an increased stiffness of this bending mode by a factor of 10 with respect to the Si–O–Si and Si–O–Al bending modes. This makes it necessary to include a bond bending term to account for the rigidity of the Si–O_H–Al angle. The form chosen here is quadratic:

$$\phi_{ijk}(\theta_{ijk}) = \tfrac{1}{2}(\theta_{ijk} - \theta_0)^2 \qquad (2)$$

The O_H force field parameters are given in Table IV, together with the previously published parameters.

The first set of parameters that was determined was based on the use of formal charge *differences* (δQ = 1), between Al and Si, and between O and O_H. As the Mulliken charge analysis of electron distribution in clusters indicates that the actual charge separation between Si and Al is much less pronounced, we derived an additional force field which assumes charge differences that have half the formal values. This is the second force field in Table IV.

Finally, a set of force fields has been developed that may be used for a "bare" aluminosilicate, i.e., without external compensating charge. In this case, we assume that the negative charge that is introduced by the aluminum atom is compensated by a slight increase in the silicon charge. Two consistent Si/Al/O force fields have been derived for charge separations of 0.48 and 0.96 between aluminum and silicon. All force fields, given in Table IV, have been fit to the same ab initio potential energy surface as the one used to determine the generic (δQ = 1) force field. Unless mentioned otherwise, the results presented were obtained with the δQ = 1 force field.

(27) Tsuneyuki, S.; Tsukada, M.; Aoki, H.; Matsui, Y. *Phys. Rev. Lett.* **1988**, *61*, 869–872.

(28) The symbol O_H is used to denote a protonated oxygen, bridging between Si and Al.

Table VI. Experimental[23] and Calculated Energy Content of Different SiO_2 Framework Topologies[a]

framework type	rings	exptl E^{rel}	CO = 10 Å n_{fr}	CO = 10 Å E	CO = 10 Å E^{rel}	CO = 5 Å n_{fr}	CO = 5 Å E	CO = 5 Å E^{rel}
coesite[30]	4	2.9	28.72	-5642.56	-1.6	27.76	-5591.76	5.4
α-quartz[31]	6	0	26.04	-5628.76	0	24.10	-5584.90	0
cristobalite[32]	6	2.8	25.02	-5612.40	11.7	19.39	-5565.14	4.0
tridymite[33]	6	3.2	19.67	-5604.56	-4.8	19.38	-5563.48	5.6
TON	5, 6		19.13	-5597.79	-0.5	17.75	-5564.56	-0.9
ZSM-48[34]	4, 5		18.77	-5597.99	-2.4	17.94	-5561.88	2.4
MTN	5, 6		17.24	-5591.60	-2.9	17.03	-5563.39	-2.2
MOR	4, 5		17.14	-5587.76	0.4	16.43	-5559.87	-0.7
ZSM-57[35]	4, 5		17.14	-5588.70	-0.5	16.89	-5560.99	-0.2
MFI	4, 5	5.5	16.95	-5591.80	-4.5	16.54	-5563.64	-4.1
LOS	4, 6		16.60	-5582.14	3.6	16.36	-5555.18	3.8
CAN	4, 6		16.59	-5582.85	2.9	16.39	-5552.96	6.1
AFI	4, 6		16.52	-5590.13	-4.7	16.28	-5555.95	2.8
SOD	4, 6		16.50	-5581.74	3.6	16.32	-5557.08	1.8
boggsite[36]	4, 5		15.13	-5581.08	-2.0	14.89	-5555.55	-1.5
CHA	4, 6		14.63	-5568.85	7.9	14.44	-5547.06	5.5
VPI-5[37]	4, 6		13.72	-5574.64	-2.0	13.57	-5548.63	1.0
LTA	4, 6		13.60	-5568.92	3.2	13.47	-5543.93	5.4
FAU	4, 6		12.61	-5564.41	3.2	12.75	-5541.67	5.2
bss[38]	4, 6		12.61	-5564.45	3.1	12.46	-5541.64	4.3
stishovite[39]	b	51.9	43.65	-5644.27	64.7	42.60	-5575.38	71.5
ZSM-18[40]	3, 4 ($^1/_5$)		13.90	-5567.38	6.1	13.73	-5544.58	5.6
LOV	3, 4 ($^2/_3$)		16.90	-5562.11	25.0	16.01	-5535.73	22.1
3^4-sodalite	3, 8 (3)		7.31	-5471.20	72.2	7.26	-5460.93	67.6

[a] The three-letter acronyms refer to structure types from the *Atlas of Zeolite Structure Types* (ref 1). References to other structures are given explicitly; 3^4-sodalite is a hypothetical framework discussed in the text. The two smallest rings within the structure are given. The figure in parentheses denotes the number of three-ring structures per SiO_2 unit. Results are presented for two different cutoffs (CO) of the short-range interaction. E^{rel} is the (corrected) energy difference with respect to α-quartz. The correction scheme is discussed in the text. Experimental results are by Johnson et al.[23] All energies are in kilojoules per mole of SiO_2. [b] Stishovite contains 6-coordinated Si.

Table VII. Energy Content of Different $AlPO_4$ Polymorphs, Using a 10-Å Cutoff[a]

framework type	rings	C.O. = 10 Å n_{fr}	E	E^{cor}
berlinite[41]	6	24.52	-5716.59	0
AEL	4, 6	18.35	-5693.12	0.7
AFI	4, 6	15.87	-5688.74	-5.0
SOD	4, 6	15.84	-5683.20	0.5
ERI	4, 6	14.95	-5676.27	4.0
VPI-5[37]	4, 6	13.49	-5676.71	-1.9
FAU	4, 6	12.11	-5668.97	0.6

[a] Symbols and units are the same as in Table II.

Table VIII. Relaxation Energy (kJ/mol Al) of an Aluminum Substitution in a Silica Four Ring (ab Initio, 3-21G) and in Faujasite (Molecular Mechanics)[a]

ab initio system	ab initio δE	force field system	force field δQ	force field δE
4R-Al	114.3	FAU-Al	0.96	107.0
			0.48	61.1
4R-AlNa	129.2	FAU-AlNa	1.00	119.3
4R-AlO_H	211.4	FAU-AlO_H	1.00	304 ● 9
			0.50	262 ± 8

[a] For FAU-AlO_H, the numbers are averaged over all possible O_H substitution sites.

2.3. Lattice Energy Minimization Calculations. Rigid-ion lattice energy minimization results were obtained by constant-pressure energy minimization. In this method,[29] both atomic positions and unit cell parameters are varied till the net force on all atoms is zero. The long-range Coulomb interaction is evaluated via the Ewald summation; the short-range interactions are truncated at a cutoff radius of 10 Å. The Si–O_H–Al bond bending term is evaluated only for the two T atoms nearest to the O_H group. In all cases, the experimental structure was used as a starting point. Care is taken to ensure that optimized structures correspond to energy minima by checking that all vibrational frequencies are positive. Therefore, the minimum-energy structures correspond to stable (global) minima. This is confirmed by a molecular dynamics study by Tsuneyuki et al., who show that a force field of the type used here produces thermodynamically stable SiO_2 polymorphs.[27]

For the twenty-four SiO_2 polymorphs listed in Table VI and the seven $AlPO_4$ polymorphs listed in Table VII, an energy minimization has been performed, starting from the experimental crystal geometries. The term 3^4-sodalite refers to a hypothetical structure (supersodalite), obtained by replacing the Si atoms by Si_4O_6 tetrahedra consisting of four fused three-ring structures (hence, 3^4). For the SiO_2 systems, additional calculations were performed with a 5-Å cutoff radius, to probe the effect of truncation of the short-range potential. For all structures, we have tabulated the smallest ring(s) that can be identified, the framework density of the energy-minimized structure and the total energy content. Additionally, the relative energy with respect to α-quartz (E^{rel}) is given. These numbers have been corrected for a spurious dependence on the framework density, following a scheme that will be presented in section 2.4.

As indicated in the Introduction, acidic zeolites that are of catalytic interest have part of the silicon atoms replaced by aluminum or other trivalent cations. We will consider here the isomorphous substitution of silicon by aluminum. The framework of the resulting aluminosilicate becomes negatively charged. Replacement of silicon by aluminum in a free cluster induces considerable changes in the interatomic distances and angles, as can be seen from the data on geometry-optimized small clusters, given in Table III.

With a view to probing the structural relaxation of an aluminum substitution embedded in an infinite lattice, lattice energy minimizations

(29) Catlow, R. C. A.; Mackrodt, W. C. In *Computer Simulation of Solids*; Catlow, R. C. A., et al., Eds.; Lecture Notes in Physics 166; Springer Verlag: Berlin, 1982; pp 3–21.
(30) Levien, L.; Prewitt, C. T. *Am. Mineral.* **1981**, *66*, 324.
(31) Levien, L.; Prewitt, C. T.; Weidner, D. J. *Am. Mineral.* **1980**, *65*, 920.
(32) Peacor, D. P. *Z. Kristallogr.* **1973**, *138*, 274.
(33) Wyckoff, R. W. G. *Crystal Structures*; Interscience: New York, 1963; Vol. 1.
(34) Schlenker, J. L.; Rohrbaugh, W. J.; Chu, P.; Valyocsik, E. W.; Kokotailo, G. T. *Zeolites* **1985**, *5*, 355–358.
(35) Schlenker, J. L.; Higgins, J. B.; Valyocsik, E. W. *Abstracts of Papers*, 8th International Zeolite Conference, Amsterdam, July 1989; p 287.
(36) Pluth, J. J.; Smith, J. V.; Howard, D. G.; Tschernich, R. W. *Abstracts of Papers*, 8th International Zeolite Conference, Amsterdam, July 1989; p 111.
(37) Davis, M. E.; Saldarriaga, C.; Montes, C.; Garces, J.; Crowder, C. *Zeolites* **1988**, *8*, 362.
(38) Hexagonal modification of faujasite (Breck structure 6), from Breck, D. W. *Zeolite Molecular Sieves*; Wiley: New York, 1974; p 57.
(39) Bauer, W. H.; Kahn, A. A. *Acta Crystallogr.* **1971**, *B27*, 2133.
(40) Lawton, S. L.; Rohrbaugh, W. J. *Science* **1990**, *247*, 1319–1322.
(41) Schwarzenbach, D. *Z. Kristallogr.* **1966**, *123*, 161.

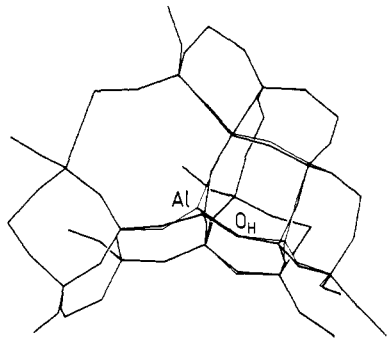

Figure 2. Local geometry of a AlO_H substitution in faujasite. The heavy lines indicate the bonds in the structure of all-silica faujasite; the thin lines represent the relaxed structure of the AlO_H-substituted faujasite. The figure extends up to the third Si-coordination shell around the Al substitution.

were performed on faujasite with one aluminum substitution per unit cell of 48 T atoms.[42] The reference structure was all-silica faujasite (FAU-Si) as determined by lattice energy minimization with the force field of Table IV. The difference in formal charge between 4-coordinated silicon and aluminum renders the framework negatively charged. To compensate for this charge, we will consider three models that are analogous to the three quantum chemical models.

In the first model (FAU-Al), the compensating charge is distributed over all remaining silicon atoms. This corresponds to the physical situation where the compensating charge is spread out evenly over space. This makes the model insensitive to the precise location of the compensating charge. Two calculations have been performed with different charge separations between Si and Al (δQ = 0.48 and 0.96). This allows us to check the sensitivity of our answers with respect to variations in the degree of covalency or ionicity of the system. The force fields, discussed in the previous section, are given in Table IV. Table VIII lists the relaxation energies for each of these force fields. The relaxation energy is defined as the energy difference between the aluminum substitution in the FAU-Si structure and that in the fully relaxed structure.

The second model (FAU-AlNa) has a sodium ion to compensate for the negative framework charge. In a first calculation, the Na^+ position is optimized with respect to the framework that has the FAU-Si geometry. This calculation provides the energy reference value of the unrelaxed structure. Subsequently, the structure is fully optimized to obtain the energy of the relaxed system.

Finally, in the third model, we consider substitution of aluminum combined with the attachment of a proton to a neighboring oxygen atom. The model (FAU-AlO_H) has four realizations, because of the four different oxygen atoms with the asymmetric unit of faujasite. The results on relaxation energy and relaxed structure are averaged over the four substituted configurations.

The resulting relaxation energies (δE) are given in table VIII; structural parameters, such as bond distances and angles, for the various models are given in Table III. Figure 2 shows a graphic representation of the framework relaxation around one of the Al/OH substitutions in faujasite. Note that the lattice distortion is much localized, i.e., confined almost to nearest neighbors of Al and O_H. As seen from Table III, the local geometry resembles very closely the optimized geometry of the $(OH)_3Si$–(OH)–$Al(OH)_3$ cluster.

2.4. Energy Correction Scheme. In Figure 3, we have plotted the energy content of twenty SiO_2 polymorphs built from four-, five-, and six-ring structures and seven $AlPO_4$ polymorphs versus the framework density. One observes that, in all data sets, there is a linear dependence between the two quantities. Such a relation was absent in the results obtained with empirical potentials.[18] Below, we will argue that the density dependence of the lattice energy, shown in Figure 3, is a spurious consequence of the potential energy functions chosen. We will see that, once a correction has been made, there is a nice correspondence between force field results and quantum chemical results, on the one hand, and between force field results and experimental data, on the other.

The potential energy functions (Table IV) have been derived from the potential energy surface of small clusters (single and double tetrahedrons) and information on the structure and elastic properties of α-quartz. The ab initio cluster information provides a gauge for the interatomic interaction energy at small (intra cluster) distances; the information on α-quartz was used to optimize the force field predictions of structure and

(42) The smallest possible unit cell was chosen, having $a = b = c \approx 17.5$ Å and $\alpha = \beta = \gamma = 60°$ and containing 48 T atoms.

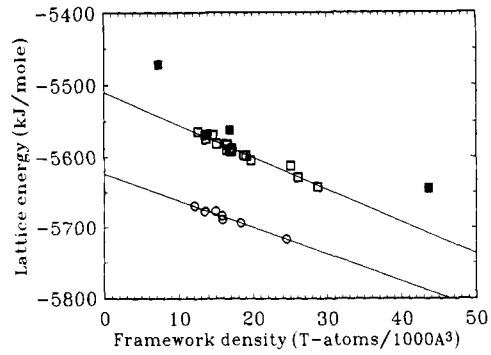

Figure 3. Total energy content (from Tables VI and VII of the twenty-four SiO_2 and seven $AlPO_4$ polymorphs), plotted versus the calculated framework density n_{fr}. Regular four-, five-, and six-ring-containing polymorphs are indicated with open squares (SiO_2) and open circles ($AlPO_4$); the solid squares denote three-ring structures and stishovite. The drawn lines represent the linear density dependence of the framework energy (eqs 6 and 8), which is shown to be a spurious consequence of the r^{-6} term in the force field.

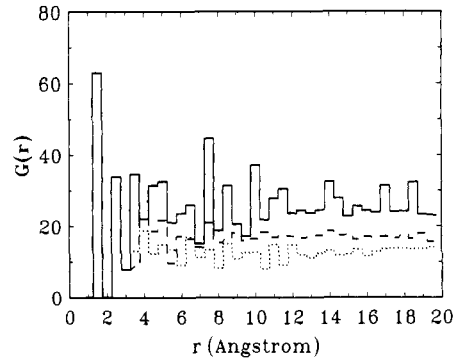

Figure 4. A histogram of the atom–atom correlation function $G(r)$ (eq 4) for quartz (drawn line), mordenite (large dashes), and faujasite (small dashes). At small distances, $G(r)$ is the same for all compounds, reflecting the fact that the atomic coordination is identical for all compounds; beyond 4 Å, $G(r)$ rapidly tends to the bulk density n_{fr}.

elastic properties, and to remove the parameter redundancy remaining in the fit to cluster data. Tentatively, one may associate the fine tuning of force field parameters through comparison with bulk data with the adjustment of interactions between tetrahedrons. Beyond these distances (typically beyond next-nearest tetrahedron), the *forces* from individual atoms will effectively cancel each other because of the isotropy of the system, while the *energy contributions* are additive. The above considerations imply that the potential energy contribution of the interaction between distant atoms need not have any physical significance. In summary, energy terms stemming from nonelectrostatic interactions between atoms that are more than 3–4 Å apart may cause systematic errors in the total energy results. Its specific cause and subsequent correction are discussed below.

Let us consider the effect of the potential energy terms of eq 1 one by one. The exponential short-range repulsion term is of no concern, since its rapid decay causes it to be of no importance at larger distances. On the opposite end of the spectrum, the long-range Coulomb forces will yield reasonable Madelung energies, since the calculated atomic positions are in good agreement with experiment. Hence, the only uncertainty is its magnitude, which scales with atomic charges.

However, a problem is presented by the r^{-6} attraction term of the potential energy function. As discussed in a previous paper,[22] this term is not related to the van der Waals attraction between atoms; its function here is entirely empirical: It adjusts the interatomic interactions at small distances. The c_{ij} values used are much higher than the values estimated for the true van der Waals interaction between atoms. The latter may be assessed by substituting atomic values for the polarizability α_i[43] and ionization energy I_i[44] into the London expression:[45]

$$c_{ij} = {}^3/_2 \frac{\alpha_i \alpha_j I_i I_j}{I_i + I_j} \qquad (3)$$

(43) Miller, T. M.; Bederson, B. In *Advances in Atomic and Molecular Physics 13*; Bates, D. R., et al., Eds.; Academic Press: New York, 1977; pp 1–57.

Values of 6.6, 41, 33, and 25 eV Å^6 result for the O–O, Al–O, Si–O, and P–O interactions, respectively, up to 30 times less than those used in the force field (Table IV).

It is this overestimation of the r^{-6} term that leads to a spurious density dependence of the total energy. Figure 4 shows the atom–atom pair correlation function, $G(r)$, for α-quartz and zeolites MOR and FAU. We have defined $G(r)$ as

$$G(r) = \frac{1}{4\pi r^2 N} \sum_{i=1}^{N} \sum_{j} \delta(|\vec{r}_i - \vec{r}_j| - r) \quad (4)$$

where i runs over all N atoms in a unit cell. Note that the first coordination shells are identical for all systems. Beyond 4 Å, $G(r)$ is system-dependent and rapidly converges to the bulk density n_{fr}. As a consequence, the lattice energy contains a contribution, $\Phi_6^>(\bar{R})$, which is linearly dependent on the framework density:

$$\Phi_6 = \Phi_6^<(\bar{R}) + \Phi_6^>(\bar{R}) = \sum_{i,j(r_{ij}<\bar{R})} \frac{c_{ij}}{r_{ij}^6} + \sum_{i,j(\bar{R}<r_{ij}<R_{CO})} \frac{c_{ij}}{r_{ij}^6} =$$

$$\Phi_6^<(\bar{R}) - \sum_{\lambda_i\lambda_j} \int_{\bar{R}}^{R_{CO}} \frac{c_{\lambda_i\lambda_j} G_{\lambda_i\lambda_j}(r)}{r^6} \, d\vec{r} \approx$$

$$\Phi_6^<(\bar{R}) - (2c_{OO} + c_{SiO}) \int_{\bar{R}}^{R_{CO}} \frac{n_{fr}}{r^6} \, d\vec{r} =$$

$$\Phi_6^<(\bar{R}) - \frac{4\pi}{3}(2c_{OO} + c_{SiO}) \left\{ \frac{1}{\bar{R}^3} - \frac{1}{R_{CO}^3} \right\} n_{fr} \quad (5)$$

$G_{\lambda_i\lambda_j}(r)$ is the type-selective pair correlation function, defined as in eq 4, and λ runs over all atom types; R_{CO} and $\bar{R}$ denote the cut-off radius and the physically relevant range of the r^{-6} term, respectively.

The relation between framework density and lattice energy as found in the energy minimizations of the 21 "regular" SiO_2 frameworks is accurately described by the relation

$$E = -5509.612 - 4.55639 n_{fr} \quad (6)$$

for the calculations with a cutoff radius of 10 Å and by the relation

$$E = -5502.218 - 3.34876 n_{fr} \quad (7)$$

when a 5-Å cutoff radius is used. Energies are in kilojoules per mole of SiO_2, and the framework density is in Si atoms per 1000 Å^3. The difference between the 10 and 5 Å slopes ($1.20 n_{fr}$) should be accounted for by r^{-6} contributions from pairs of atoms that are between 5 and 10 Å apart. Using eq 5 with $\bar{R}$ = 5 Å, we calculate $1.37 n_{fr}$, thus corroborating the idea that the density dependence stems from the r^{-6} term. Taking this idea one step further, we may calculate the value for $\bar{R}$ that would eliminate the density dependence completely. One finds that $\bar{R}$ = 3.45 and 3.41 Å for the data sets obtained by using R_{CO} = 10 and 5 Å, respectively. This value for $\bar{R}$ corresponds with the next-next-nearest neighbor distance. If one subtracts this spurious contribution to the energy, the total energy content for all silica networks is the same to within 10 kJ/mol and essentially independent of framework density.

The data for a series of $AlPO_4$ polymorphs show exactly the same trend. Energy contents for berlinite and six microporous $AlPO_4$ networks are given in Table VII. The optimal relation between energy content and framework density is

$$E = -5623.860 - 3.79207 n_{fr} \quad (8)$$

for R_{CO} = 10 Å. The slope can be correlated with the slope of the SiO_2 systems: Their ratio should, according to eq 5, be given by

$$\frac{4c_{OO} + 2c_{SiO}}{4c_{OO} + c_{AlO} + c_{PO}} = 1.14 \quad (9)$$

in reasonable agreement with the ratio between the slopes in eqs 6 and 8 (4.56/3.79 = 1.20). The remaining differences in lattice energies between the polymorphs are less than 10 kJ/mol TO_2, identical with the spread in the SiO_2 energies.

The theoretical predictions for SiO_2 polymorphs are compiled in Figure 5, where a comparison is made with experimental data of Johnson et al.[23] It is gratifying that the prediction for stishovite correlates so well with experiment. As argued in a previous paper,[22] the accuracy with which our force field models this compound, which has Si coordinated by six oxygen atoms, should be attributed to the range of deformation of the $Si(OH)_4$ cluster that has been used to construct the potential energy surface to which the potentials have been fitted.

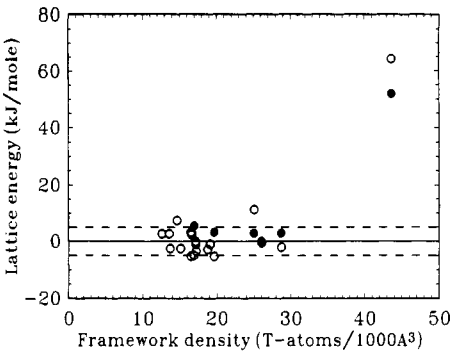

Figure 5. Calculated (open circles) and observed (solid circles) total energy contents (from Table VI and ref 23) of the 20 regular SiO_2 polymorphs and stishovite, versus the framework density. The calculated points have been corrected for the framework density.

3. Discussion

The data presented above enable a comparison between the properties of small, isolated building blocks of zeolites, as calculated by ab initio quantum chemistry, and the properties of the same clusters embedded in an infinite zeolite lattice. The latter calculations used a force field approach, but we assured its validity by gauging the potentials to the ab initio determined potential energy surface of small clusters.

It appears that the energy contents of four-, five-, and six-ring structures are very close to one another. The maximum deviation found in the ab initio calculations is 4 kJ/mol SiO_2. This energy difference is small enough for all species to be thermodynamically accessible both at ambient temperature and at the zeolite synthesis temperature. This finding had already been reported earlier,[18] but the extent to which the energy of small building blocks is indicative of the energy of an infinite lattice was not known. Preliminary results obtained with empirical SiO_2 potentials indicated energy differences of up to 40 kJ/mol SiO_2.[18] The lattice energies as found with the present force field revealed a remarkable relation between energy and framework density. We have shown that this is due to an artefact of the force field. Removal of the spurious density dependence renders the energy content of all four-, five-, and six-ring networks equal to within 10 kJ/mol SiO_2. One may conclude that the secondary building blocks of the zeolite framework (specifically rings) are easily accommodated in the framework; i.e., the resulting strain is less than 10 kJ/mol SiO_2. It is worthwhile to mention that the 40 kJ/mol differences found with empirical force field are retained upon the application of the correction scheme of section 2.4, because the r^{-6} terms in this force field are much smaller.

Indeed, this conclusion is further substantiated by the results of microporous networks with three-ring structures. Three networks are considered: ZSM-18, the recently synthesized zeolite containing one three-ring structure per unit cell; Lovdarite (LOV), which exhibits so-called spiro-five-ring structures and exists only in a beryllium-containing form, and a hypothetical zeolite (3^4-sodalite), which has the sodalite structure with all the T atoms replaced by Si_4O_6 tetrahedra. The corrected energies of these systems are 6–70 kJ/mol SiO_2 higher than those of the four-, five-, and six-ringed systems. If one calculates the excess energy per three-ring unit, one finds that any three-ring unit contributes 25–35 kJ/mol silicon atoms that are part of one three-ring structure, in good agreement with the 30 kJ/mol SiO_2, found in the 3-21G level ab initio results on free clusters.[46] In conclusion, the 3-ring structures that are strained when considered as free entities have quantitatively the same strain when embedded in an extended system.

(44) *Handbook of Chemistry and Physics 64*; Weast, R. C., et al., Eds.; CRC Press: Boca Raton, FL, 1983; p E-63.

(45) Pitzer, K. S. *Adv. Chem. Phys.* **1959**, *2*, 59.

(46) Since the force field parameterization was done on the basis of ab initio results using a 6-31G basis, it is fair to make the quantitative comparison with the 3-21G results, rather than with the STO3G results.

The magnitude of the excess energy associated with three-ring structures is such that is seems highly unlikely, if not impossible, that SiO_2 polymorphs can be synthesized with a large number of three-ring units in the structure. Incorporation of other framework elements may lift this prohibition, as indicated by the presence of beryllium in the spiro-five-ring structure of lovdarite and by the 3^4 units found in germanium sulfides.[25]

The other question that can be answered on the basis of a comparison of ab initio and force field results relates to the geometric relaxation around an aluminum substitution in an all-silica lattice. Resolving the local structure around such a substitution is of great importance for our understanding of the acidity of zeolites. A recent paper by Corbin et al.[47] provides experimental evidence for the extreme flexibility of the zeolite lattice (in that case, zeolite RHO). In their work, the researchers are not able to discriminate between silicon and aluminum atoms. Instead, they work with effective T atoms. Only in the case of zeolites with a 1:1 Si:Al ratio, does the Si/Al ordering induced by Löwensteins avoidance rule enable a structure refinement where one can discriminate between Al and Si. For low aluminum loadings, such structural refinement is impossible. It is here that accurate theoretical modeling can be of help.

In nature, charge compensation comes either from protons, attached to (neighboring) oxygen atoms, or from cations (e.g., Na^+) in the pores of the zeolites. In our calculations, these possibilities are covered by the model systems 4R-AlO_H and FAU-AlO_H, respectively, 4R-AlNa and FAU-AlNa. Additionally, we have considered the case where charge compensation is completely delocalized (4R-Al and FAU-Al). A study of Table III reveals a remarkable feature of all models. The local geometry changes that occur near an aluminum substitution are virtually the same in the cluster models as in the extended models. In spite of the long-range electrostatic forces within zeolites, which we explicitly account for in our force field model, the reconstruction of the lattice is a purely local phenomenon. This spatial confinement is also illustrated by Figure 2.

A rationale for the above lies in the order of magnitude difference between the bond stretching and bond bending of the Si–O–Si and Si–O–Al angles. Whereas the Si–O distances are invariant from one zeolite to the next, the Si–O–Si angle varies between 130 and 180°, to allow vastly different network topologies and structures. Just as the angles change from one zeolite to the next, so do they upon substitution of a framework atom: The distance differences are accommodated in the infinite network by a slight adjustment of the next angle on oxygen.

The coupling between the locality of distortions and the weakness of the Si–O–Si bond bending implies that the reliability of the results depends primarily on the accuracy with which this bond bending is accounted for in the force field. Previous work[22] indicates that the vibrational frequencies that correspond to bond bending are predicted slightly too high by the force field. This would imply that, in reality, the above-described effect of accommodation of distance differences by bond bending is even stronger.

Apart from insight into the geometry of a framework substitution, we have obtained information on the relaxation energy of substitutions. The data of Table VIII show the same ordering of relaxation energies for different models of charge compensation within the ab initio and the force field approach. Perhaps the most striking thing about the relaxation energies is their similarity in the cluster models and extended structures. The predicted relaxation energies of the 4R-Al and FAU-Al, as well as the 4R-AlNa and FAU-AlNa models, are mutually the same to within 10 kJ/mol Al. This points (i) to the reliability of the force field and (ii) to the freedom of the embedded cluster. For the models that have an acid proton as the charge-compensating entity, the correspondence is somewhat less, but the discrepancy is significantly reduced if one lowers the charge separation δQ between Al and O_H from 1.0 to 0.5. The latter value is in better agreement with the Mulliken charges found in the ab initio calculations on the 4R-AlO_H model. The difference by a factor of 2 in relaxation energies between Al and AlNa models on the one hand ($\delta E \approx$ 100 kJ/mol) and the AlO_H models on the other ($\delta E \approx 200$ kJ/mol) can be correlated with the number of T centers that are distorted: one (the Al center) in the case of Al and AlNa and two (Al and Si_{OH}) in the AlO_H case.

In conclusion, just as in the all-silica systems, the Al-containing zeolites can accommodate ring structures virtually without strain. The structural relaxation induced by the appreciable bond length differences remain local; the relaxation energy involved is approximately 100 kJ/mol per distorted T site.

The evidence compiled in this paper for the comparative "freedom" of embedded aluminosilicate clusters has important consequences for the value that can be attached to various quantum chemical results on aluminosilicate clusters. The foremost conclusion is that quantum chemical calculations on small, geometry-optimized clusters provide a good basis for the study of electronic properties of zeolites, attachment of acid protons, etc. As shown in this paper, it is essential to include relaxation effects when isomorphous framework substitution or proton attachment is studied. The very presence of relaxation causes the site of disturbance to behave as in isolated geometry-optimized clusters.

This idea is completely opposite to the reasoning behind the calculations on substitutional energy by Derouane and others,[15-17] who calculate differences in substitution energy from quantum chemical calculations on clusters with the "experimental" geometry. This implies a complete neglect of the relaxability of the zeolite lattice, which we have shown to be overridingly important.

4. Conclusion

A combination of quantum chemical calculations on (alumino)silicate clusters and force field calculations on extended systems reveals that small clusters are virtually strainlessly embedded within an extended system, which justifies their use as model systems for the theoretical study of zeolites.[48]

In the case of all-silica systems, we have shown that all experimentally known four-connected silica polymorphs have lattice energies that are the same to within 10 kJ/mol, not much different from the energy differences found between four-, five-, and six-ring clusters, and in accordance with the few experimental data. All-silica three-ring clusters are energetically less favorable, which might explain their absence in nature.

The freedom of substructures was shown to have important consequences for the deformation of the silica lattice around an aluminum substitution. This work is a first attempt to give a realistic theoretical description of these distortions. It was found that the relaxation is very local. Locally, the Al–O bonds adopt the same length as in a cluster, due to the flexibility of the Si–O–Si and Si–O–Al angles.

(47) Corbin, D. R.; Abrams, L.; Jones, G. A.; Eddy, M. M.; Harrison, W. T. A.; Stucky, G. D.; Cox, D. E. *J. Am. Chem. Soc.* **1990**, *112*, 4821–4830.

(48) A recent review of theoretical work on aluminosilicate clusters is given in Sauer, J. *Chem. Rev.* **1989**, *89*, 199–255.